Small-angle neutron scattering investigation of the response of model polyurethane ionomers to uniaxial deformation

Susan A. Visser*, Gerfried Pruckmayr† and Stuart L. Cooper‡
Department of Chemical Engineering, University of Wisconsin – Madison, Madison, WI 53706, USA
†DuPont Chemicals, Chestnut Run Plaza, Wilmington, DE 19880-0709, USA
(Received 26 June 1991; revised 6 December 1991; accepted 9 December 1991)

The deformation behaviour of the poly(tetramethylene oxide) subchains of two sodium sulphonated model polyurethane ionomers is examined by small-angle neutron scattering (SANS). Surprisingly, the scattering patterns from both ionomers remained isotropic at low elongations. At higher elongations, visible anisotropy appeared in the SANS patterns, but the change in the radii of gyration in the directions parallel and perpendicular to the stretching direction was small. Three models of network deformation—the junction affine, the phantom network and the affine deformation model—failed to reproduce the experimental results. A two-stage deformation model comprising an initial stage of aggregate rearrangement and subchain relaxation at low elongations, followed by subchain stretching at higher elongations, is postulated to explain the observed results.

(Keywords: SANS; polyurethane; ionomers; deformation)

INTRODUCTION

In a previous paper[1], the response of the ionic aggregates of model polyurethane ionomers to deformation was investigated. The deformation was shown to be affine for low elongations when a 2000 molecular weight poly(tetramethylene oxide) (PTMO) soft segment was used and non-affine for all elongations of a model polyurethane ionomer based on 1000 molecular weight PTMO and for high elongations of an ionomer based on 2000 molecular weight PTMO. The non-affine response of the ionomers made evaluation of models of ionomer morphology difficult and emphasized the need to further probe the deformation response of ionomers by examining the behaviour of the polymer chains.

Small-angle neutron scattering (SANS) is one of the most powerful tools for examining the conformation of polymer chains in the solid state. Selective labelling of polymer chains with deuterium allows determination of the single-chain dimensions of the deuterated polymer in a hydrogenous polymer matrix. This technique has been used successfully to characterize the chain dimensions of ionomer backbones in carboxy-telechelic polystyrene ionomers[2], styrene/methacrylic acid ionomers[3] and model polyurethane ionomers[4]. SANS has also been used to derive information on chain dimensions in deformed systems, including polybutadiene[5], poly(dimethylsiloxane)[6], and polyisoprene[7] networks, and poly(methyl methacrylate)[8] and polystyrene[9,10] homopolymers, and styrene/isoprene triblock[11] and bisphenol A carbonate/dimethylsiloxane[12] copolymers. However, the deformation response of ionomer chains has not been studied, despite the interesting behaviour which would be expected because of the pseudo-network character of the ionomer solid state.

In this paper, the deformation responses of two sulphonated model polyurethane ionomers based on 1000 and 2000 molecular weight PTMO soft segments are studied. These polymers are well-suited for this study in several respects. They contain a regular placement of ionic groups along the polymer backbone, giving rise to a more regular morphology than is found in random copolymer ionomers[13,14]. Therefore, interpretation of the SANS data should be less complicated by artifacts of an irregular morphology. SANS data on the backbone chain dimensions of the undeformed ionomers has appeared previously[4]. Finally, the response of these ionomers to deformation has been studied by i.r. dichroism[15] and small-angle X-ray scattering (SAXS)[1], providing information which is complementary to that available by SANS.

EXPERIMENTAL

Sample preparation

Synthesis of the deuterous PTMO from fully deuterous monomer (99.5 + atom% D, Aldrich) has been described previously[16]. The hydrogenous PTMO samples were DuPont Terathanes. The molecular weight distributions

* Present address: Eastman Kodak Company Research Laboratories, Rochester, NY 14650, USA
‡ To whom correspondence should be addressed

0032-3861/92/204280-08

Table 1 Average molecular weights of PTMO polyols

Polyol	M_n	M_w	M_z
H-PTMO(1200)	1180	1769	2512
D-PTMO(1200)	1265	1725	2328
H-PTMO(2000)	1926	3344	4956
D-PTMO(2000)	1955	3168	4622

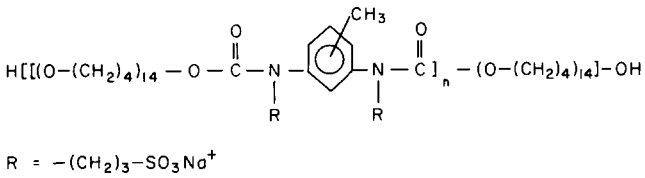

R = $-(CH_2)_3-SO_3Na^+$

Figure 1 Structure of the model polyurethane ionomer, using a 1000 molecular weight PTMO polyol as an example (n is the overall degree of polymerization)

of the hydrogenous and deuterous PTMO samples were determined by h.p.l.c.[16]. The molecular weight moments are listed in *Table 1*.

The synthesis of the polyurethane ionomers based on 1:1 copolymers of PTMO and tolylene diisocyanate (TDI) has been described previously[17]. The chemical structure of the model polyurethane ionomers is shown in *Figure 1*. The volume fraction of deuterous PTMO used in each ionomer was 25%. This labelling level has been shown[4] to satisfy the 'contrast-matched' condition[18] so that only single-chain scattering is evident in the scattering data. Polymers synthesized by this method have been shown[17] to have polystyrene-equivalent molecular weights in excess of 50 000. Sodium-neutralized sulphonate groups were introduced by replacing the urethane nitrogens with sodium propyl sulphonate groups. Elemental analysis (Galbraith Laboratories) for sulphur indicated >90% substitution at the urethane linkages for all the ionomers. The ionomers were compression moulded at 180°C for 5 min at 69 MPa and allowed to cool in the mould to room temperature overnight. Sample thicknesses were in the range 1–1.5 mm.

A five digit code was used to identify the ionomer samples. The first three letters indicate the soft segment type (M = PTMO), the soft segment molecular weight in thousands and the sulphonate pendant anion. The final two letters are the chemical symbol for the neutralizing cation. Thus, M1SNa indicates a 1:1 copolymer of PTMO, molecular weight 1000, and TDI which is derivatized at the urethane linkages with propyl sulphonate groups and stoichiometrically neutralized with sodium.

SANS measurements

The SANS data were acquired on the small-angle diffractometer at the Intense Pulsed Neutron Source at Argonne National Laboratory. Data were acquired in 67 time slices of approximately constant relative time increment ($\Delta t/t$). Samples were uniaxially extended to elongation ratios $\lambda > 1$ ($\lambda = L/L_0$, where L_0 is the distance between two marks on the unstretched sample and L is the distance for the stretched sample) using a stretching jig placed in the neutron beam path. Samples were stretched to the desired elongation ratio and allowed to relax in the new stretched configuration for at least 30 min prior to data collection. All data were collected at room temperature.

The data were corrected for empty beam scattering, spectral intensity, sample thickness and transmittance, and detector sensitivity in each time slice. The isotropic data were radially averaged and combined to yield scattering data over the q range 0.01–0.4 Å^{-1}. The anisotropic data were sector-averaged using software available at IPNS to yield scattering data over the same q range in directions parallel and perpendicular to the stretch direction. The data were placed on an absolute scale by comparison with a partially labelled polystyrene standard[19]. Incoherent background scattering was removed as described previously[4].

THEORETICAL BACKGROUND

The single chain scattering from a two-phase partially labelled polymer can be described by the equation[18]:

$$R_L(q) - R_{inc,L}(q) - \left\{\frac{[\beta_A - x\beta_{BD} - (1-x)\beta_{BH}]^2}{(\beta_A - \beta_{BH})^2} \times [R_U(q) - R_{inc,U}(q)]\right\} = \frac{4\pi}{V_S}(b_{BD} - b_{BH})^2 N_{BT} Z_B^2 x(1-x) P_B(q) \quad (1)$$

where $q = (4\pi/\lambda)\sin\theta$ is the magnitude of the scattering vector (λ is the wavelength and 2θ is the scattering angle). In equation (1), R denotes the absolute scattering cross-section or Rayleigh factor. $R_L(q)$ and $R_U(q)$ are the absolute scattering contributions from a partially labelled sample and a completely unlabelled sample. $R_{inc,L}$ and $R_{inc,U}$ are the incoherent background scattering terms for the labelled and unlabelled samples. β_A is the coherent scattering length density of pure A segments; β_{BH} and β_{BD} are the coherent scattering length densities for pure protonated and pure deuterated B segments, respectively; and x is the fraction of B chains that are deuterated. b_{BH} and b_{BD} are the monomeric coherent scattering lengths for protonated and deuterated monomers, N_{BT} is the total number of B chains present in the scattering volume, and Z_B is the average degree of polymerization of the B segments. $P_B(q)$ is the single chain scattering function, also known as the structure or form factor for the B segments or as the intramolecular interference function.

The technique of contrast matching[20] allows considerable simplification of equation (1). In this case, a labelling level is selected such that the prefactor of the second term on the left-hand side of equation (1) is equal to zero. The coherent scattering can then be described by[21]:

$$I(q) \sim (b_{BD} - b_{BH})^2 N_{BT} Z_B^2 x(1-x) P_B(q) \quad (2)$$

This equation has been shown to be valid for both uncrosslinked polymers[18,22–24] and polymer networks[25] containing a high fraction of deuterated chains.

It should be noted that equation (2) is not strictly valid when a molecular weight mismatch between hydrogenous and deuterous species exists. In that case[25,26], a Zimm representation in the low q range allows evaluation of a mean square radius of gyration

$R^2_{g,app}$:

$$P^{-1}(q) \approx 1 + \frac{q^2 R^2_{g,app}}{3} \quad \text{for } q^2 R^2_{g,app} \ll 1 \qquad (3)$$

In the case of anisotropic samples, a similar equation can be applied[27]. By analysing the intensities in the directions parallel ($q_\parallel$) and perpendicular ($q_\perp$) to the stretching direction, the component of the radius of gyration in these two main directions is obtained by:

$$P_k^{-1} \approx 1 + q^2 R_k^2 \qquad k = \parallel \text{ or } \perp \qquad (4)$$

These two components, $R_{g,\parallel}$ and $R_{g,\perp}$, can also be calculated as a function of the extension ratio λ, considering the theoretical network deformation models: junction affine deformation, phantom network deformation and affine deformation.

Models of network deformation

The junction affine deformation model assumes that deformation of the elastic chains is induced by displacement of the crosslinks, which is affine in the macroscopic deformation. This model is commonly invoked in the statistical mechanical description of elastic free energy of an isolated chain in a network[28–30]. The deformation is characterized by the relations[31,32]:

$$\frac{R_{g,\parallel}}{R_{g,0}} = \alpha_\parallel = \left(\frac{\lambda^2}{2}\right)^{1/2} \qquad (5)$$

$$\frac{R_{g,\perp}}{R_{g,0}} = \alpha_\perp = \left(\frac{\lambda + 1}{2\lambda}\right)^{1/2} \qquad (6)$$

where $R_{g,0}$ is the component of the radius of gyration of the network chains in the undeformed systems.

The deformation equations for the phantom networks, networks composed of volumeless chains that interact only at the crosslinks, have non-affine components. Pearson[33] has calculated $\alpha_\parallel$ and $\alpha_\perp$ for a uniaxially stretched phantom network. The equations depend on the functionality of the crosslinks f:

$$\frac{R_{g,\parallel}}{R_{g,0}} = \alpha_\parallel = \left[\frac{f + 2 + (f-2)\lambda^2}{2f}\right]^{1/2} \qquad (7)$$

$$\frac{R_{g,\perp}}{R_{g,0}} = \alpha_\perp = \left[\frac{f + 2 + (f-2)\lambda^{-1}}{2f}\right]^{1/2} \qquad (8)$$

For affine deformation, in which deformation of each chain segment is affine in the macroscopic deformation, the following relations hold:

$$\frac{R_{g,\parallel}}{R_{g,0}} = \alpha_\parallel = \lambda \qquad (9)$$

$$\frac{R_{g,\perp}}{R_{g,0}} = \alpha_\perp = \lambda^{-1/2} \qquad (10)$$

The classic theories of elasticity do not consider this model, but the morphological models derived for analysing the SAXS data of deformed ionomers[1] assumed affine deformation so that this model must be considered.

Polydisperse worm-like chain model for analysis of isotropic data

In order to allow comparison of the results for the isotropic samples with previously published SANS results for model polyurethane ionomers[4], the isotropic samples were also analysed using a polydisperse worm-like chain model. In this model, the scattering from the blend of hydrogenated and deuterated chains is described as[26]:

$$S(q)^{-1} = S_D(q)^{-1} + S_H(q)^{-1} - 2\chi \qquad (11)$$

where χ is the Flory interaction parameter and $S_i(q)$, i = H or D, are the scattering contributions from the hydrogenous and deuterous subchains, respectively:

$$S_i(q) = v_i \int_{N_i=0}^{N_i=\infty} \omega_i g(u_N) N_i \, dN_i \qquad (12)$$

where N_i is the degree of polymerization of oligomer of isotope type i, ω_i is the weight fraction of oligomer i (relative to all material of isotope type i) and v_i is the volume fraction of material of isotope type i. [To simplify notation, the subscripts i will be dropped for all quantities except $S_i(q)$, recognizing that both isotope types must be evaluated in equation (12).] $g(u_N)$ is the structure factor of the polymer chain, given by [34]:

$$g(u_N) = \frac{2}{u^2}(e^{-u} + u - 1) + \frac{2}{5q^2L^2} \times [-11u\,e^{-u} + 4u + 7(1 - e^{-u})] \qquad (13)$$

where L is the contour length of the chain ($L = nl$, where n is the number of monomers in the chain and l is the contour length of a monomer unit). Here, u_N is given by:

$$u_N = q^2 R^2_{g,N} = q^2 n_N a^2/6 = q^2 N l a/6 \qquad (14)$$

where $R_{g,N}$ is the radius of gyration of chain length N, a is the statistical segment length and n_N is the number of statistical segments. Using tabulated bond lengths and angles, the monomer contour length for PTMO can be calculated[35] to be 6.11 Å.

To analyse the SANS data with this model, equations (11)–(14) were used directly with the h.p.l.c. data[4], which describes the molecular weight distribution of the PTMO subchains. The statistical segment or Kuhn length[36] a was a fitting parameter. The contrast factor relating $S(q)$ to the absolute intensity $I(q)$ is:

$$I(q) = \frac{(\Delta\beta)^2 m_0 v_L}{\rho N_A} S(q) \equiv K S(q) \qquad (15)$$

where $\Delta\beta$ is the scattering length density difference between hydrogenous and deuterous PTMO ($\Delta\beta = 6.82 \times 10^{10}$ cm^{-2}), m_0 is the monomer molecular weight ($m_0 = 72.11$ g mol^{-1}), ρ is the amorphous PTMO mass density (0.98 g cm^{-3})[37] and N_A is Avogadro's number. v_L is the volume fraction of the chain that can be labelled; v_L is around 0.8 for the ionomers examined here, giving $K = 0.454$ cm^{-1}. K is treated as a fitting parameter to account for any errors in absolute intensity calibration. The Flory interaction parameter χ is taken as zero; variation of χ from zero would have little effect on the results, as noted by Register *et al.*[38].

RESULTS AND DISCUSSION

The two-dimensional contour plots of the neutron scattering from the undeformed ($\lambda = 1$) and deformed ($\lambda > 1$) M1SNa and M2SNa ionomers appear in *Figures 2* and *3*. The scattering patterns of the undeformed ionomers are clearly isotropic, but surpris-

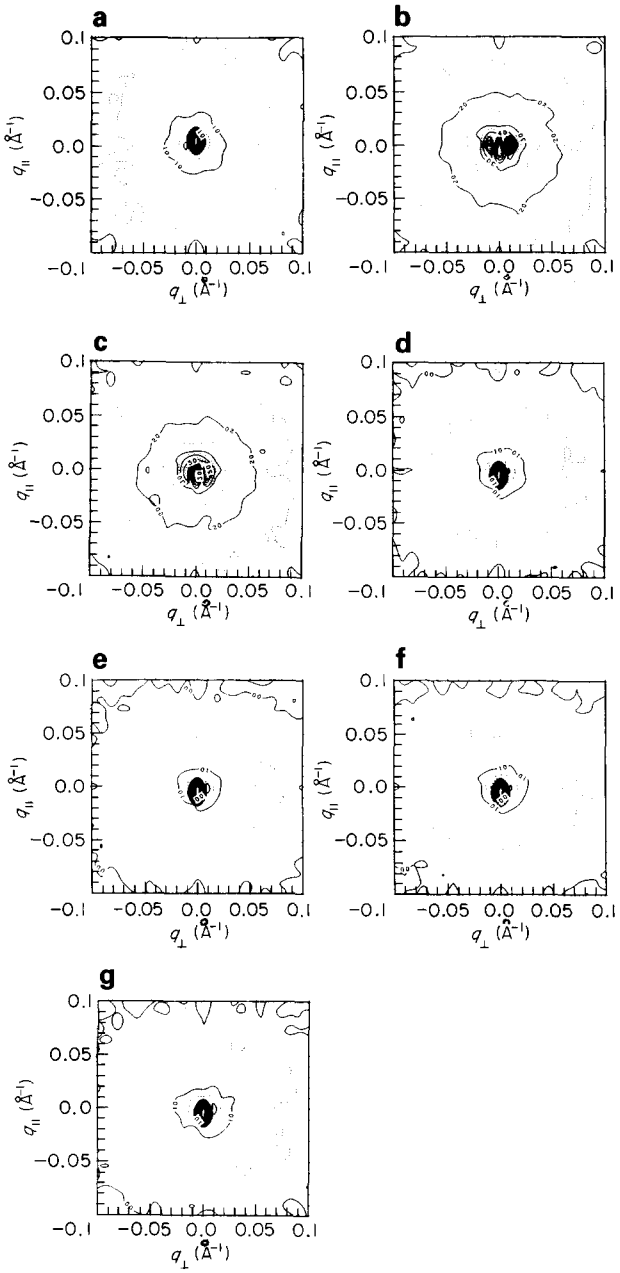

Figure 2 Two-dimensional contour plots of SANS data for M1SNa at various elongation ratios: λ = (a) 1.0; (b) 1.25; (c) 1.5; (d) 1.75; (e) 2.0; (f) 2.5; (g) 3.0. The stretching direction is vertical

ingly, the scattering patterns of the M1SNa ionomers up to elongation ratios $\lambda = 1.75$ and of the M2SNa ionomers up to elongation ratios $\lambda = 2.0$ are also isotropic. Beginning at $\lambda = 1.75$ for M1SNa and $\lambda = 2.0$ for M2SNa, the contour patterns display increasing ellipsoidal eccentricity as λ is increased, indicating an increase in the orientation of the PTMO chains. The onset of anisotropy in the scattering patterns, as well as its extent at a given value of λ, is greater for the M1SNa ionomer than for M2SNa, indicating a higher degree of orientability for the M1SNa subchains. Even at the highest elongations examined, however, the degree of anisotropy of the scattering patterns remains relatively slight, suggesting that the response of the PTMO subchains to the external deformation is attenuated by rearrangements in the ionomer microstructure. The M2SNa ionomer, having half the ionic group concentration of the M1SNa ionomer, has more freedom to undergo rearrangements, explaining the apparent delay in its response to the external deformation compared to M1SNa.

The data from the ionomers giving isotropic scattering patterns were initially analysed using the worm-like chain model described by equations (11)–(15). The modelling results appear in *Table 2* and *Figure 4*. Within experimental error, the results for the undeformed samples precisely match results obtained previously on M1SNa and M2SNa ionomers[4]. For M1SNa, increasing the elongation ratio up to a value of $\lambda = 1.5$ had no effect on the measured $R_{g,z}$ within experimental error. For M2SNa, although the isotropic nature of the scattering pattern was maintained up to $\lambda = 2.0$, the measured $R_{g,z}$ increased slightly as λ increased from 1.00 to 1.50. The slight increase in $R_{g,z}$ may be a reflection of the redistribution of the ionic aggregates which could cause local swelling of the polymer chains without inducing visible anisotropy in the single-chain scattering. (No evidence of two-phase scattering appeared in any of the scattering patterns, indicating that the 'contrast-matched' condition was maintained for all samples and that scattering from voids did not contribute to the observed scattering.)

In order to permit comparison to the results for ionomers giving anisotropic scattering patterns, data for ionomers with isotropic scattering patterns were also analysed using the Zimm-type analysis described by equation (3). *Figure 5* shows Zimm plots for M1SNa; similar plots were derived for M2SNa (data not shown).

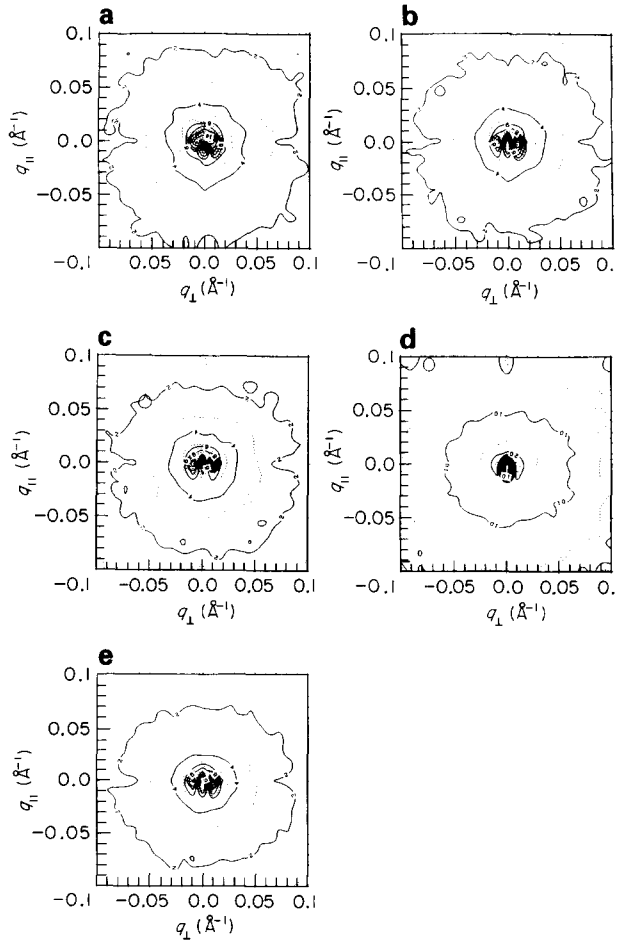

Figure 3 Two-dimensional contour plots of SANS data for M2SNa at various elongation ratios: λ = (a) 1.0; (b) 1.5; (c) 2.0; (d) 2.5; (e) 3.0. The stretching direction is vertical

Table 2 Worm-like chain modelling results for isotropic samples

Sample	λ	a (Å)	K (cm^{-1})	$R_{g,z}$ (Å)
M1SNa	1.00	15.2 ± 1.3[a]	0.438 ± 0.009[a]	22.6
M1SNa	1.25	17.0 ± 1.3	0.412 ± 0.008	23.8
M1SNa	1.50	17.1 ± 1.6	0.417 ± 0.009	23.9
M2SNa	1.00	12.7 ± 0.7	0.506 ± 0.008	29.0
M2SNa	1.50	14.3 ± 0.8	0.496 ± 0.008	30.8
M2SNa	2.00	14.4 ± 0.9	0.488 ± 0.009	30.9

[a] ±SD

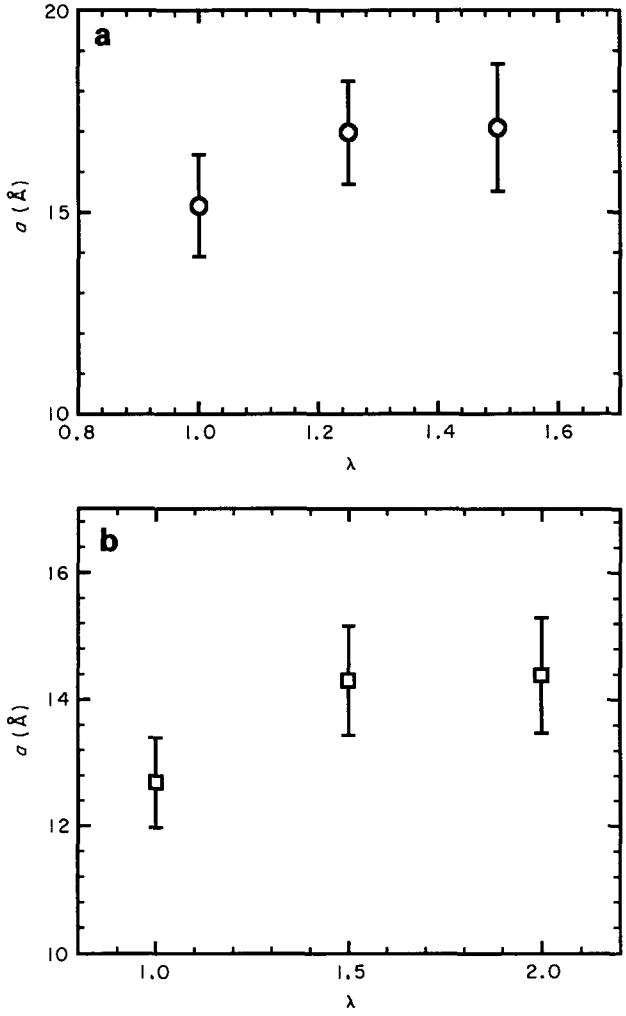

Figure 4 Variation of statistical segment length a with elongation ratio λ for (a) M1SNA and (b) M2SNa ionomers whose scattering patterns remain isotropic

The linearity of the Zimm plots reaffirms the validity of this type of analysis. Results are given in *Table 3* and indicate that R_g remains constant in these samples. (Slight but significant changes were noted in the worm-like chain analysis for M2SNa because that model uses a wider range of data. This allows a greater statistical sampling to be modelled and a smaller standard deviation to be estimated.)

Equations (3) and (4) are valid for mixtures of deuterated and hydrogenated polymer of identical molecular weights. In the systems investigated here, the molecular weight distributions of the deuterous and hydrogenous species are not strictly the same (see *Table 1*).

It follows that the radius of gyration calculated with equations (3) and (4) is an apparent value. An analysis of the error introduced by using these equations on polydisperse systems, following the method of Boue *et al.*[26], indicates that the relative errors for M1SNa and M2SNa are $<1\%$ and are therefore negligible.

Results of the analysis for the M1SNa samples giving anisotropic scattering patterns appear in *Figures 6* and *7* and *Table 4*. Examination of *Figure 6* shows that the slope of the Zimm plots for scattering parallel to the stretching direction ($q_\parallel$) for $\lambda = 1.75$, 2.0, 2.5 and 3.0 varies little, indicating that $R_{g,\parallel}$ varies little with λ, even at these higher elongations. In contrast, scattering of the M1SNa ionomers in the perpendicular direction ($q_\perp$), shown for the higher elongations in *Figure 7*, shows a definite change in the slope of the Zimm plot as λ increases. Referring to *Table 4*, the trend appears to be that $R_{g,\perp}$ increases as λ increases, matching the qualitative conclusions that can be drawn from examination of *Figure 2*. However, the error limits prevent attaching any significance to this trend in the Zimm analysis.

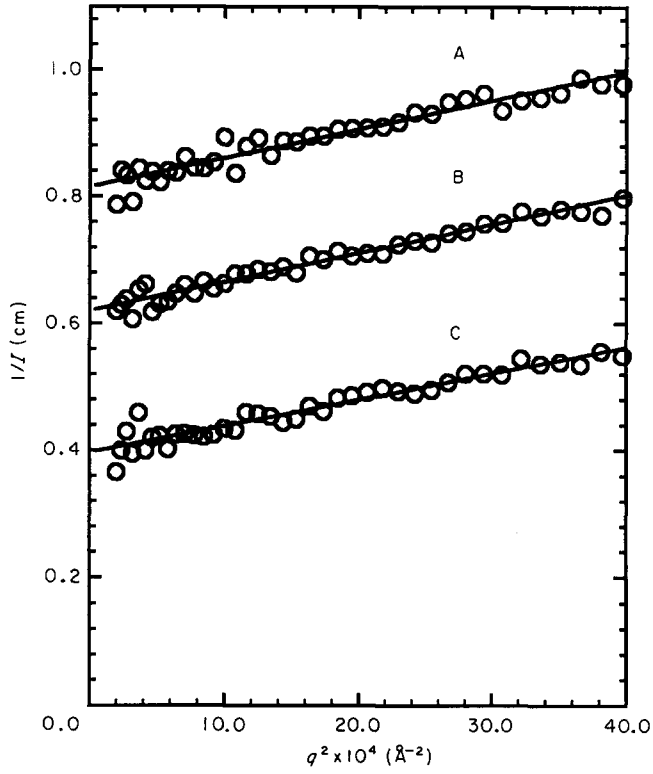

Figure 5 Zimm plots of isotropic scattering data which resulted in isotropic scattering patterns at various elongation ratios λ for M1SNa. λ = (A) 1.5; (B) 1.25; (C) 1.0. Curves at elongation ratios of $\lambda > 1$ have been incrementally offset by 0.2 cm in $1/I$ for clarity

Table 3 Zimm analysis results for samples giving isotropic scattering patterns

Sample	λ	R_g (Å)
M1SNa	1.00	17.7 ± 1.3
M1SNa	1.25	18.0 ± 1.0
M1SNa	1.50	18.1 ± 1.2
M2SNa	1.00	25.3 ± 1.1
M2SNa	1.50	25.9 ± 1.0
M2SNa	2.00	26.5 ± 1.0

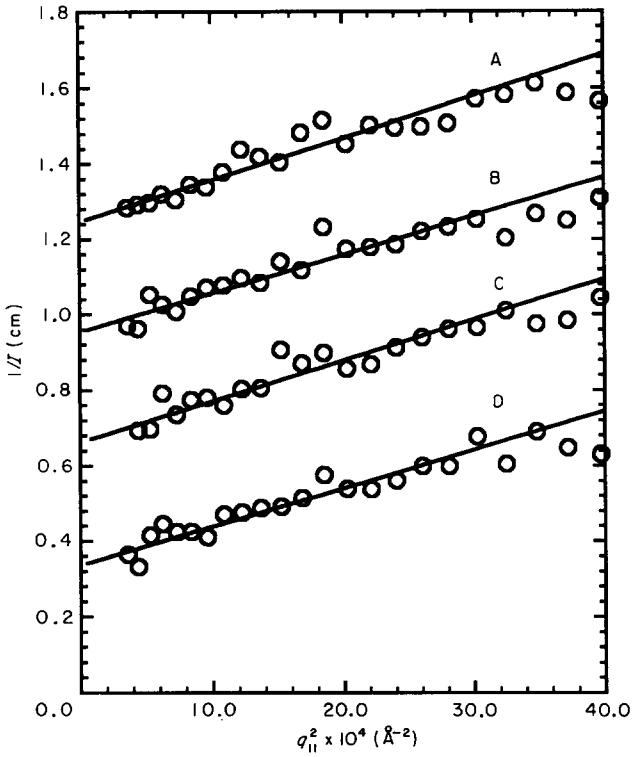

Figure 6 Zimm plot of anisotropic scattering data for M1SNa in the direction parallel to the stretching direction. λ = (A) 3.0; (B) 2.5; (C) 2.0; (D) 1.75. Curves at elongation ratios of $\lambda \geqslant 2.0$ have been incrementally offset by 0.3 cm in $1/I$ for clarity

Table 4 Zimm analysis results for samples giving anisotropic scattering patterns

Sample	λ	$R_{\parallel}$ (Å)	$R_{\perp}$ (Å)	R_g[a] (Å)
M1SNa	1.75	17.4 ± 2.1		15.2
M1SNa	1.75		14.0 ± 1.7	
M1SNa	2.00	17.3 ± 1.9		15.9
M1SNa	2.00		15.2 ± 1.8	
M1SNa	2.50	17.1 ± 2.0		15.0
M1SNa	2.50		13.9 ± 1.5	
M1SNa	3.00	17.9 ± 1.5		14.5
M1SNa	3.00		12.5 ± 2.2	
M2SNa	2.00	18.6 ± 1.4		18.1
M2SNa	2.00		17.8 ± 1.2	
M2SNa	3.00	19.4 ± 1.4		19.1
M2SNa	3.00		18.9 ± 1.4	

[a] For samples which displayed anisotropy, R_g values were calculated from:

$$R_g^2 = \frac{2R_{\perp}^2 + R_{\parallel}^2}{3}$$

Significant differences between $R_{g,\perp}$ and $R_{g,\parallel}$ at $\lambda = 3.0$ are noted in the Zimm analysis.

The variation of molecular deformation with λ is plotted in *Figure 8*, as are the predictions from the three network deformation models. Clearly, the deformation of the PTMO subchains of M1SNa is highly non-affine. The junction affine model also fails to predict the slight changes in $R_{g,i}$ which were observed. In order to obtain the best possible fit of the experimental data to the phantom network model, it was necessary to postulate a crosslink functionality of three. Previous SAXS studies of the ionic aggregates of similar ionomers indicate that a minimum of 20 ionic groups reside in each aggregate[14] so that this postulation violates known facts of ionomer morphology. Further, even if the postulation of a crosslink functionality of three could be justified based on the number of ionic groups dispersed in the matrix (estimated at up to 50% in some ionomers[39]), the crosslink functionality must still be greater than three. Use of crosslink functionality values greater than three

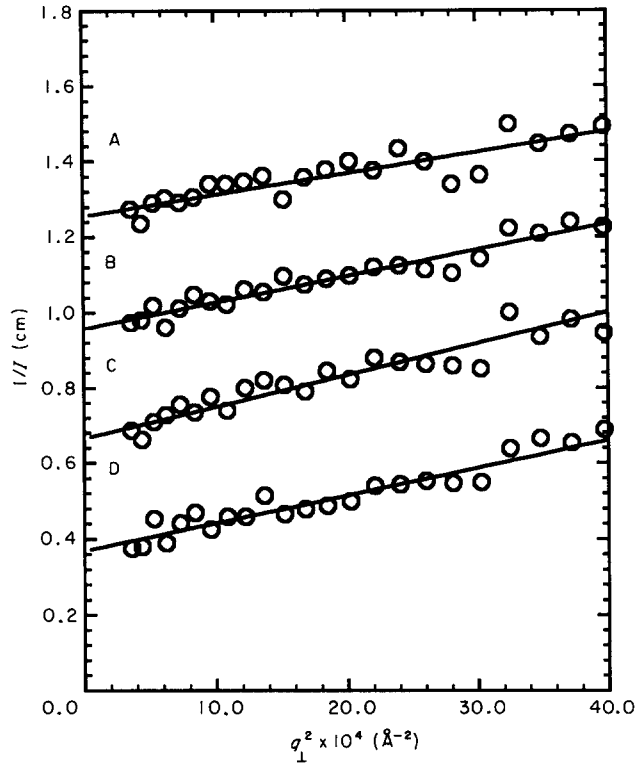

Figure 7 Zimm plot of anisotropic scattering data for M1SNa in the direction perpendicular to the stretching direction. λ = (A) 3.0; (B) 2.5; (C) 2.0; (D) 1.75. Curves at elongation ratios of $\lambda \geqslant 2.0$ have been incrementally offset by 0.3 cm in $1/I$ for clarity

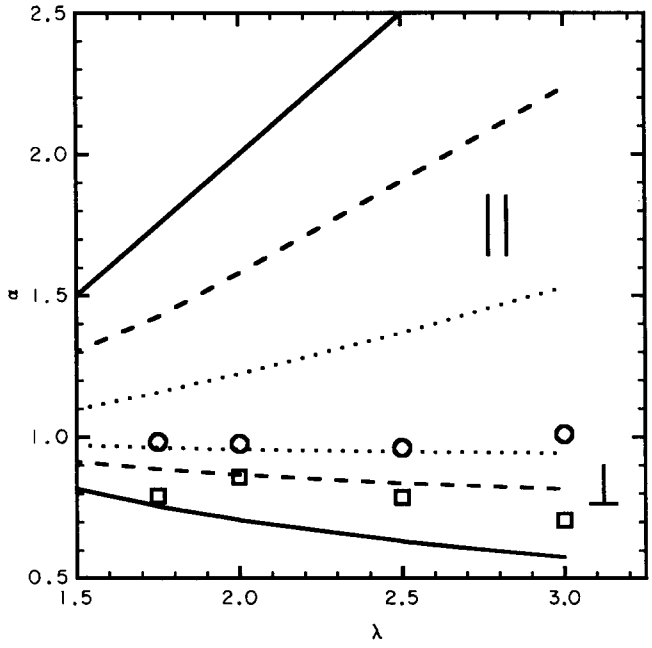

Figure 8 Variation of molecular deformation α in the direction parallel (○) and perpendicular (□) to the stretching direction for M1SNa and comparison to the three models of network deformation: (——) affine; (– – –) junction affine; (· · ·) phantom network ($f = 3$)

gives even greater discrepancies between experimental results and model predictions.

The anisotropic scattering results for the M2SNa ionomers are shown in *Table 4*. The Zimm plots (not shown) display little variation in slope as λ is increased, indicating no significant changes in $R_{g,\perp}$ and $R_{g,\parallel}$ as λ increases from 2.0 to 3.0.

Comparing the scattering results for M1SNa and M2SNa, the largest variation of R_g was observed for ionomers with the shortest subchains. In neither the M1SNa nor the M2SNa case was the deformation affine. These results match the conclusions reached for deformation of chemically crosslinked poly(dimethylsiloxane) networks[6], confirming the validity of the analogy between physically crosslinked networks of ionomers and chemically crosslinked networks of non-ionic polymers.

A more detailed understanding of the response of ionomers to deformation is obtained by comparison of the SANS results with previously published SAXS analyses of deformed M1SNa and M2SNa ionomers[1]. The SAXS results showed a significant variation in the position of the scattering peak in q-space up to a value of $\lambda = 1.75$ for M1SNa. At elongations of $\lambda > 1.75$, the peak position in the directions parallel and perpendicular to the stretching direction remained approximately constant. This change in response is exactly paralleled by the response seen in the SANS data, where the onset of anisotropy in the SANS patterns occurred at $\lambda = 1.75$ for M1SNa. From consideration of these data, it can be postulated that two processes affect the subchain deformation behaviour. At elongations below $\lambda = 1.75$, the deformation is characterized by rearrangement of the ionic aggregates in the polymer matrix, resulting in a shift in the SAXS peak position. (The peak must, therefore, arise from interparticle interference. See reference 1 for an explanation of the implications of this statement.) The rearrangement of the crosslink points allows the deformation of the PTMO subchains to lag behind the macroscopic deformation, explaining the isotropic nature of the neutron scattering for the slightly elongated samples. At higher elongations ($\lambda \geqslant 1.75$), the aggregate rearrangement is unable to permit complete subchain relaxation, and stretching of the PTMO subchains begins to be observed. This deformation mechanism is also supported by the M2SNa data. The SAXS peak position for M2SNa changes its position in q-space up to $\lambda = 2.0$, precisely the elongation at which anisotropy becomes apparent in the SANS patterns. An initial period of aggregate rearrangement, followed by subchain stretching at higher elongations, also explains the M2SNa scattering results.

The later (higher λ) onset of anisotropy in the scattering patterns of M2SNa than of M1SNa is explained by the lower number of crosslink points on each M2SNa chain. A greater number of crosslink points per chain would limit the mobility of the chains and therefore of the ionic aggregates. Relaxation of the PTMO subchains through aggregate redistribution would be less in the M1SNa ionomers, resulting in the onset of anisotropy in the scattering patterns at lower elongations.

CONCLUSIONS

The response to uniaxial deformation of the PTMO subchains of sodium sulphonated model polyurethane ionomers was examined. Despite the pseudo-network character of the ionomers, the M1SNa and M2SNa ionomers both exhibited continued isotropic scattering at low elongations. Scattering at higher elongations revealed the onset of a small degree of anisotropy in the scattering patterns, but the deformations were clearly non-affine. The largest variation of R_g was observed for the ionomers with the shortest PTMO subchains and, therefore, the highest ionic group concentrations. This resulted from the increased anchoring effect of the larger number of ionic groups; the M1SNa ionomer subchains were more closely tied to the macroscopic deformation of the system.

Reference to previously published SAXS results allowed the deformation mechanism of these ionomers to be divided into two stages. In the first stage, at low elongations, the ionic aggregates underwent redistribution in the polymer matrix, allowing the PTMO subchains to relax so that continued isotropic neutron scattering was observed. At higher elongations, the aggregate redistribution was insufficient to allow complete relaxation of the PTMO subchains so that the subchains began to show response to the macroscopic deformation. Subchain stretching, as evidenced by the appearance of anisotropy in the SANS patterns, was observed.

Because of the unusual two-stage deformation mechanism of the ionomers, the three models of network deformation (affine, junction affine and phantom network) were unable to model the scattering results. In all cases, the increase in R_g predicted by the models greatly exceeded that observed experimentally. Internal relaxations and rearrangements of the ionic aggregates explain the discrepancies.

ACKNOWLEDGEMENTS

This work has benefited from the use of the Intense Pulsed Neutron Source at Argonne National Laboratory which is funded by the US Department of Energy, BES-Materials Science, under Contract W-31-109-ENG-38. Support for this work was provided by the US Department of Energy through Grant DE-FG02-88ER45370, and by the donors of the Petroleum Research Fund, administered by the American Chemical Society, through Grant 20343-AC7. SAV gratefully acknowledges the fellowship support of the American Association of University Women Educational Fund in the form of an Engineering Dissertation Fellowship.

REFERENCES

1 Visser, S. A. and Cooper, S. L. *Macromolecules*, 1992, **25**, 2230
2 Register, R. A., Cooper, S. L., Thiyagarajan, P., Chakrapani, S. and Jerome, R. *Macromolecules* 1990, **23**, 2978
3 Pineri, M. Duplessix, R., Gauthier, S. and Eisenberg, A. *Adv. Chem. Ser.* 1980, **187**, 283
4 Visser, S. A., Pruckmayr, G. and Cooper, S. L. *Macromolecules* 1991, **24**, 6769
5 Hinckley, J. A., Han, C. C., Mozer, B. and Yu, H. *Macromolecules* 1978, **11**, 836
6 Beltzung, M., Picot, C. and Herz, J. *Macromolecules* 1984, **17**, 663
7 Yu, H., Kitano, T., Kim, C. Y., Amis, E. J., Chang, T., Landry, M., Wesson, J. A., Han, C. C., Lodge, T. P. and Glinka, C. J. *Polym. Prepr.* 1985, **26**(2), 60
8 Dettenmaier, J., Maconnachie, A., Higgins, J. S., Kausch, H. H. and Nguyen, T. Q. *Macromolecules* 1986, **19**, 773
9 Picot, C., Duplessix, R., Decker, R., Benoit, H., Boue, F.,

Cotton, J. P., Daoud, M., Farnoux, B., Jannink, G., Nierlich, A., deVries, J. and Pincus, P. *Macromolecules* 1977, **10**, 436
10 Hadziioannou, G., Wang, L. H., Stein, R. S. and Porter, R. S. *Macromolecules* 1982, **15**, 880
11 Richards, R. W. and Thomason, J. L. *Polymer* 1983, **24**, 275
12 Hammouda, B., Yelon, W. B., Lind, A. C. and Hansen, F. Y. *Macromolecules* 1989, **22**, 418
13 Ding, Y. S., Register, R. A., Yang, C.-Z. and Cooper, S. L. *Polymer* 1989, **30**, 1213
14 Visser, S. A. and Cooper, S. L. *Macromolecules* 1991, **24**, 2584
15 Ding, Y. S., Register, R. A., Yang, C.-Z. and Cooper, S. L. *Polymer* 1989, **30**, 1204
16 Andrews, G. D., Vatvars, A. and Pruckmayr, G. *Macromolecules* 1982, **15**, 1590
17 Visser, S. A. and Cooper, S. L. *Macromolecules* 1991, **24**, 2576
18 Koberstein, J. T. *J. Polym. Sci., Polym. Phys. Edn* 1982, **20**, 593
19 Jayasuriya, D. S., Tcheurekdjian, J., Wu, C. F., Chen, S. H. and Thiyagarajan, P. *J. Appl. Crystallogr.* 1988, **21**, 843
20 Quan, X. and Koberstein, J. T. *J. Polym. Sci., Polym. Phys. Edn* 1987, **25**, 1381
21 Benôit, H., Koberstein, J. and Leibler, L. *Makromol. Chem. Suppl.* 1981, **4**, 85
22 Williams, C. E., Nierlich, M., Cotton, J. P., Jannick, G., Boue, F., Daoud, M., Farnoux, B., Picot, C., deGennes, P. G., Rinauso, J., Moan, M. and Wolff, C. *J. Polym. Sci., Polym. Lett. Edn* 1979, **17**, 379
23 Wignall, G. D., Hendricks, R. W., Koehler, W. C., Lin, J. S., Wai, M. P., Thomas, E. L. and Stein, R. S. *Polymer* 1981, **22**, 886
24 Miller, J. A. and Cooper, S. L. *Makromol. Chem.* 1984, **185**, 2429
25 Beltzung, M., Picot, C., Rempp, P. and Herz, J. *Macromolecules* 1982, **15**, 1594
26 Boue, F., Nierlich, M. and Leibler, L. *Polymer* 1982, **23**, 29
27 Beltzung, M., Picot, C. and Herz, J. *Macromolecules* 1984, **17**, 663
28 Flory, P. J. and Rehner, J. *J. Chem. Phys.* 1943, **11**, 512
29 Wall, F. T. and Flory, P. J. *J. Chem. Phys.* 1951, **19**, 1435
30 Hermans, J. J. *J. Polym. Sci.* 1962, **59**, 191
31 Duplessix, R. *PhD Thesis* Universite Louis Pasteur, Strasbourg, 1975
32 Levy, S. *PhD Thesis* Universite Louis Pasteur, Strasbourg, 1964
33 Pearson, D. S. *Macromolecules* 1977, **10**, 696
34 Sharp, P. and Bloomfield, V. A. *Biopolymers* 1968, **6**, 1201
35 Weast, R. C. (Ed.) 'CRC Handbook of Chemistry and Physics', 59th Edn, CRC Press, Baco Raton, 1978
36 Kuhn, W. *Kolloid Z* 1939, **87**, 3
37 Miller, R. L. in 'Polymer Handbook, Third Edition' (Eds J. Brandrup and E. H. Immergut), John Wiley and Sons, New York, 1989, p. IV-72
38 Register, R. A., Pruckmayr, G. and Cooper, S. L. *Macromolecules* 1990, **23**, 3023
39 Yarusso, D. L. and Cooper, S. L. *Polymer* 1985, **26**, 371